

Shadows of rotating five-dimensional EMCS black holes

Muhammed Amir,^{1,*} Balendra Pratap Singh,^{1,†} and Sushant G. Ghosh^{2,3,‡}

¹*Centre for Theoretical Physics, Jamia Millia Islamia, New Delhi 110025, India*

²*Centre for Theoretical Physics, Jamia Millia Islamia, New Delhi 110025 India*

³*Astrophysics and Cosmology Research Unit, School of Mathematics,
Statistics and Computer Science, University of KwaZulu-Natal,
Private Bag X54001, Durban 4000, South Africa*

Abstract

It is known that a black hole shadow is a dark region due to the falling geodesics of photons into the black hole. We study shapes of the shadow cast by the rotating five-dimensional Einstein-Maxwell-Chern-Simons (EMCS) black holes, which is characterized by the four parameters, i.e., mass, two spins, and charge, in which spin parameters are set equal. We integrate the null geodesic equations and derive an analytical formula for the shadow of five-dimensional EMCS black hole. We also investigate the shadow cast by a black hole to show that the size of the black hole shadow is affected due to charge as well as spin. The shadow is a dark zone covered by a deformed circle, and the size of the shadow decreases with an increase in the charge q when compared with the five-dimensional Myers-Perry black hole. Interestingly, the distortion increases with charge q . The effect of these parameters on the shape and size of naked singularity shadow of five-dimensional EMCS black hole is also discussed.

PACS numbers: 04.50.Gh, 04.70.-s, 04.25.-g

*Electronic address: amirctp12@gmail.com

†Electronic address: balendra29@gmail.com

‡Electronic address: sghosh2@jmi.ac.in

I. INTRODUCTION

Black holes are intriguing astrophysical objects and are perhaps the most fascinating objects in astrophysics. It is hard to find any other object or topic that attracts more attention. However, it is still unproven whether black holes can be observed. The observation of the black hole candidate Sgr A* shadow is one of the important goals of the Very Large Baseline Interferometry (VLBI). It should be able to image the black hole with resolution at the level of the event horizon. The galactic center black hole candidate Sgr A*, due to the gravitational lensing effect, should cast a shadow; the shape and size of this shadow can be calculated. There is a widespread belief that an evidence for the existence of black holes will come from the direct observation of its ‘shadow’. The shape of a shadow could be used to study extreme gravity near the event horizon and also to know whether the general relativity is consistent with the observations. Observation of a black hole shadow may allow us to determine the mass and spin of a rotating black hole [1–5]. As black holes are basically non emitting objects, it is of interest the study null geodesics around them where photons coming from other sources move, to obtain shadow. To a distant observer, the event horizons cast shadows due to the bending of light by the black holes [6]. As a first step towards the study of a black hole shadow was by Bardeen [7], he calculated the shape of a dark area of a Kerr black hole, i.e., its ‘shadow’ over a bright background. The Schwarzschild black hole’s shadow is a perfect circle [8, 9], while the Kerr black hole doesn’t have a circular shadow image; it has elongated shape in the direction of rotation [10]. Thus, the shadow deviation from the circle, can determine the spin parameter of black holes. The study of black holes has been extended for other black holes, such as Kerr [7], Kerr-Newman [11], regular black holes [12–14], multi-black hole [15], black holes in extended Chern-Simons modified gravity [16] and Randall-Sundrum braneworld [17]. Shadows of black holes with nontrivial NUT charge were obtained in [18], while the Kerr-Taub-NUT black hole was discussed in [19]. The apparent shape of the Sen black hole is studied in [20], and rotating braneworld black holes were investigated in [17, 21]. Further, the effect of a spin parameter on the shape of the shadow was extended to the Kaluza-Klein rotating dilaton black hole [22], the rotating Horava-Lifshitz black hole [23], rotating non-Kerr black hole [24] and Einstein-Maxwell-dilaton-axion black hole [25]. There are some different approaches to calculate the shadow of the black holes, e.g., a coordinate-independent characterization [26] and general

relativistic ray-tracing [27].

Recent years witnessed black hole solutions in more than four spacetime dimensions, especially in five-dimensions as the subject of intensive research motivated by ideas in braneworld, string theory and gauge/gravity duality. Several interesting and surprising results have been found [28].

The models with large, extra dimensions have been proposed to deal with several issues arising in modern particle phenomenology [28–31]. The rotating black holes have many applications and display interesting structures, but they are also very difficult to find in higher-dimensions and the bestiary for solutions is much wider and less understood [32, 33]. The uniqueness theorems do not hold in higher-dimensions due to the fact that there are more degrees of freedom. The black-ring solution in five-dimensions shows that higher-dimensional spacetime can admit nontrivial topologies [34]. The Myers-Perry black hole solution [35] is a higher-dimensional generalization of the Kerr black hole solution. However, the Kerr-Newman black hole solution in higher-dimensions is not yet been discovered. Nevertheless, there is a related solution of the Einstein-Maxwell-Chern-Simons (EMCS) theory in the five-dimensional minimal gauged supergravity [36, 37]. The shadow of five-dimensional rotating black hole [38] suggests that the shadow is slightly smaller and less deformed than for its four-dimensional Kerr black hole counterpart. Recently, the shadow of higher-dimensional Schwarzschild-Tangherlini black holes is discussed in [39] and the results shows that the size of the shadow decreases in higher-dimensions.

The aim of this paper is to investigate the shadow of a five-dimensional EMCS minimal gauged supergravity black hole (henceforth five-dimensional EMCS black hole) and compare the results with shadow for the Kerr black hole/five-dimensional Myers-Perry black hole.

The paper is organized as follows: In Sec. II, we review the five-dimensional Myers-Perry black hole solution and also visualizes the ergoregion for various values of the charge q . In Sec. III, we have presented the particle motion around the five-dimensional EMCS black hole to discuss the shadow of the black hole. In Sec. IV two observables are introduced to discuss the apparent shape of the shadow of the black hole. The naked singularity shadow of five-dimensional EMCS black hole is subject of Sec. V and finally in Sec. VII, we have concluded the main results.

We have used units that fix the speed of light and the gravitational constant via $8\pi G = c = 1$.

II. ROTATING FIVE-DIMENSIONAL EMCS BLACK HOLES

We briefly review the five-dimensional asymptotically flat Einstein-Maxwell-Chern-Simons (EMCS) black hole solutions. The Lagrangian for the bosonic sector of the minimal five-dimensional supergravity can be described as [40, 41]:

$$\mathcal{L} = \frac{1}{16\pi} \left[\sqrt{-g}(R - F^2) - \frac{2}{3\sqrt{3}} \epsilon^{\mu\nu\rho\sigma\tau} A_\mu F_{\nu\rho} F_{\sigma\tau} \right], \quad (1)$$

where R is the curvature scalar, $F_{\mu\nu} = \partial_\mu A_\nu - \partial_\nu A_\mu$ with A_μ the gauge potential, and $\epsilon^{\mu\nu\lambda\rho\sigma}$ is the five-dimensional Levi-Civita tensor. The Lagrangian (1) has an additional Chern-Simons term than usual Einstein-Maxwell term. The corresponding Einstein field equations of motion reads [41, 42]:

$$\begin{aligned} R_{\mu\nu} - \frac{1}{2} g_{\mu\nu} R &= 2 \left(F_{\mu\alpha} F_{\nu\alpha} - \frac{1}{4} g_{\mu\nu} F_{\rho\sigma} F^{\rho\sigma} \right), \\ \nabla_\mu \left(F^{\mu\nu} + \frac{1}{\sqrt{3}\sqrt{-g}} \epsilon^{\mu\nu\lambda\rho\sigma} A_\lambda F_{\rho\sigma} \right) &= 0. \end{aligned} \quad (2)$$

A five-dimensional rotating EMCS black hole solution [41], in Boyer-Lindquist coordinates $(t, r, \theta, \phi, \psi)$ can be expressed by the metric

$$\begin{aligned} ds^2 &= -\frac{\rho^2 dt^2 + 2q\nu dt}{\rho^2} + \frac{2q\nu\omega}{\rho^2} + \frac{\mu\rho^2 - q^2}{\rho^4} (dt - \omega)^2 \\ &\quad + \frac{\rho^2 dx^2}{4\Delta} + \rho^2 d\theta^2 + (x + a^2) \sin^2 \theta d\phi^2 \\ &\quad + (x + b^2) \cos^2 \theta d\psi^2, \end{aligned} \quad (3)$$

where the gauge potential for the metric (3) can be expressed by

$$A_\mu dx^\mu = \frac{\sqrt{3}q}{\rho^2} (dt - \omega) \quad (4)$$

and

$$\begin{aligned} \Delta &= (x + a^2)(x + b^2) + q^2 + 2abq - \mu x, \\ \rho^2 &= x + a^2 \cos^2 \theta + b^2 \sin^2 \theta, \\ \nu &= b \sin^2 \theta d\phi + a \cos^2 \theta d\psi, \\ \omega &= a \sin^2 \theta d\phi + b \cos^2 \theta d\psi, \end{aligned} \quad (5)$$

where μ is related to the black hole mass, q is the charge and a, b are the two different angular momenta of the black hole. Furthermore, the non-zero components of the metric

(3), can be expressed as

$$\begin{aligned}
g_{tt} &= \frac{\rho^2(\mu - \rho^2) - q^2}{\rho^4}, \\
g_{t\phi} &= -\frac{a(\mu\rho^2 - q^2) + bq\rho^2 \sin^2 \theta}{\rho^4}, \\
g_{t\psi} &= -\frac{b(\mu\rho^2 - q^2) + aq\rho^2 \cos^2 \theta}{\rho^4}, \\
g_{\phi\psi} &= \frac{[ab(\mu\rho^2 - q^2) + (a^2 + b^2)q\rho^2] \sin^2 \theta \cos^2 \theta}{\rho^4}, \\
g_{xx} &= \frac{\rho^2}{\Delta}, \quad g_{\theta\theta} = \rho^2, \\
g_{\phi\phi} &= (x + a^2) \sin^2 \theta + \frac{a[a(\mu\rho^2 - q^2) + 2bq\rho^2] \sin^4 \theta}{\rho^4}, \\
g_{\psi\psi} &= (x + b^2) \cos^2 \theta + \frac{b[b(\mu\rho^2 - q^2) + 2aq\rho^2] \cos^4 \theta}{\rho^4}.
\end{aligned} \tag{6}$$

The radial coordinate has been changed to a new radial coordinate x via $x = r^2$. One can check that when $q = 0$, the five-dimensional EMCS black hole reduces to the five-dimensional Myers-Perry black hole [35], and also in addition to $a = 0$, it reduces to five-dimensional Schwarzschild-Tangherlini black hole [43]. It may be noted that the metric (3) is independent of the coordinates (t, ϕ, ψ) , and hence it admits three Killing vectors given by

$$\ell = \frac{\partial}{\partial t} + \Omega_a \frac{\partial}{\partial \phi} + \Omega_b \frac{\partial}{\partial \psi}, \tag{7}$$

and these killing vectors become null at the event horizon. The angular velocities for the metric (3) can be define as

$$\begin{aligned}
\Omega_a &= \frac{a(x_+ + b^2) + bq}{(x_+ + a^2)(x_+ + b^2) + abq}, \\
\Omega_b &= \frac{b(x_+ + a^2) + aq}{(x_+ + a^2)(x_+ + b^2) + abq}.
\end{aligned} \tag{8}$$

The surface gravity for the EMCS black hole (3) takes the following form [36],

$$\kappa = \frac{x_+^2 - (ab + q)^2}{\sqrt{x_+}[(x_+ + a^2)(x_+ + b^2) + abq]}. \tag{9}$$

The five-dimensional EMCS black hole obeys the first law of thermodynamics and with the help of surface gravity (9), the Hawking temperature of the black hole can be easily calculated via $T = \kappa/(2\pi)$. And the entropy of the black hole is given [36] by

$$S = \frac{\pi^2[(x_+ + a^2)(x_+ + b^2) + abq]}{2\sqrt{x_+}}, \tag{10}$$

when $a = b = 0 = q$, it reduces to

$$S = \frac{\pi^2 x_+^{3/2}}{2}. \quad (11)$$

The Komar integrals reads

$$J = \frac{1}{16\pi} \int_{S^3} *dK, \quad (12)$$

where $K = \partial/\partial\phi$ or $K = \partial/\partial\psi$, yielding

$$J_a = \frac{\pi(\mu a + qb)}{4}, \quad J_b = \frac{\pi(\mu b + qa)}{4}. \quad (13)$$

The electric charge can be calculated by the Gaussian integral,

$$Q = \frac{1}{16\pi} \int_{S^3} (*F - F \wedge A/\sqrt{3}), \quad (14)$$

which gives

$$Q = \frac{\sqrt{3}\pi q}{4}. \quad (15)$$

As we know the five-dimensional EMCS black hole follows the first law of thermodynamics so the conserved mass or the energy can be calculated by integrating

$$dE = TdS + \Omega_a dJ_a + \Omega_b dJ_b + \Phi dQ, \quad (16)$$

where Φ is the electrostatic potential and by integrating above equation, we find the conserved energy as

$$E = \frac{3\pi\mu}{8}, \quad (17)$$

which represents the conserved energy of the five-dimensional EMCS black hole. Interestingly, the determinant is the same as in the uncharged case $\sqrt{-\det g} = \rho^2 \sin\theta \cos\theta/2$.

A. Horizons and ergosphere

Our aim is to discuss the effect of q on the horizons and also on the ergosphere. It can be seen that the metric (3) is singular at $\rho^2 = 0$ and $\Delta = 0$. As $q = 0$, the five-dimensional EMCS black hole is reduced to the five-dimensional Myers-Perry black hole which is analyzed

in [35, 38]. Note that $\rho^2 = 0$ is a physical singularity and $\Delta = 0$ gives a coordinate singularity which defines the horizons of the metric (3). It turns out that $\Delta = 0$, admits two roots [41]

$$x_{\pm}^H = \frac{1}{2} \left(\mu - a^2 - b^2 \pm \sqrt{(\mu - a^2 - b^2)^2 - 4(ab + q)^2} \right), \quad (18)$$

which correspond to five-dimensional EMCS black hole with two regular horizons, the event horizon (x_+^H) and the Cauchy horizon (x_-^H), when $(\mu - a^2 - b^2)^2 > 4(ab + q)^2$ or $\mu > (a + b)^2 + 2q$ [41]. It represents an extremal black hole with degenerate horizons ($x_+^H = x_-^H$) when $\mu = (a + b)^2 + 2q$, and a naked singularity when $\mu < (a + b)^2 + 2q$. If $q = 0$, the Eq. (18) takes the following form:

$$x_{\pm}^H = \frac{1}{2} \left(\mu - a^2 - b^2 \pm \sqrt{(\mu - a^2 - b^2)^2 - 4(ab)^2} \right), \quad (19)$$

where both of roots shows the two horizons of the Myers-Perry spacetime [35, 38]. If we consider, the case when both the spin parameters are equal, i.e., $a = b$, then the Eq. (18) reduces to

$$x_{\pm}^H = \frac{1}{2} \left(\mu - 2a^2 \pm \sqrt{(\mu - 2a^2)^2 - 4(a^2 + q)^2} \right). \quad (20)$$

In this case the extremal black hole occurs at $\mu = 2(2a^2 + q)$, a naked singularity occurs at $\mu < 2(2a^2 + q)$, and a non-extremal black hole exists at $\mu > 2(2a^2 + q)$. Thus the black hole charge affects the horizon structure when $q = 0$, the Eq. (20) reduces to

$$x_{\pm}^H = \frac{1}{2} \left(\mu - 2a^2 \pm \sqrt{(\mu - 2a^2)^2 - 4a^4} \right). \quad (21)$$

which shows the two non degenerate horizons of five-dimensional Myers-Perry black hole [35, 38] for equal rotation parameter. Another feature of any rotating black hole is the presence of a so-called static limit surface. Next, we find static limit surface where the time-like Killing vectors of the metric become null, i.e., $g_{tt} = 0$, which leads to

$$(x + a^2 \cos^2 \theta + b^2 \sin^2 \theta)^2 - \mu(x + a^2 \cos^2 \theta + b^2 \sin^2 \theta) + q^2 = 0, \quad (22)$$

which can be trivially solves to [41]

$$x_{\pm}^{sls} = \frac{1}{2} \left(\mu \pm \sqrt{\mu^2 - 4q^2} \right) - a^2 \cos^2 \theta - b^2 \sin^2 \theta, \quad (23)$$

for equal rotation parameter $a = b$ [41], roots can be defined as

$$x_{\pm}^{sls} = \frac{1}{2} \left(\mu \pm \sqrt{\mu^2 - 4q^2} \right) - a^2. \quad (24)$$

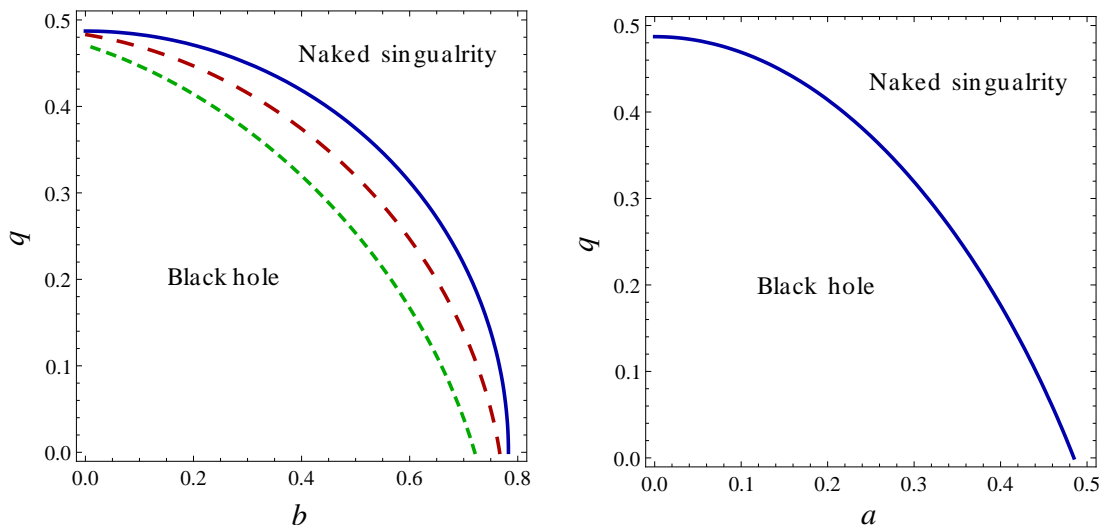


FIG. 1: Plot showing the dependence of charge q with spin a, b . (Left) For $a \neq b$, $a = 0$ (blue solid line), $a = 0.1$ (red dashed line), $a = 0.2$ (green dashed line). (Right) For $a = b$.

We see that in the limit $q \rightarrow 0$,

$$x_+^{sls} = \mu - a^2, \quad x_-^{sls} = a^2. \quad (25)$$

It can be seen that both the surfaces, i.e., static limit surface and the horizons of the black hole are not coinciding at the poles ($\theta = 0, \pi/2$), and hence the ergosphere is totally different from the Kerr-Newman where they do coincide at the poles (cf. Fig. 2). The only possibility is that when we have chosen [41]

$$\theta = \arccos \left(\pm \sqrt{\frac{\mu}{a^2 + b^2}} \right), \quad \text{and} \quad q = -\frac{ab\mu}{a^2 + b^2}.$$

Hence, for the above values of θ and q , both surfaces of the metric (3) coincide. Figure 1 shows the contour plots of $\Delta = 0$, for the cases when $a \neq b$ and $a = b$. The contours depicted in Fig. 1 indicate the boundary lines between a black hole region and the naked singularity. The coinciding roots arise on the colored line and there exists two roots inside the black hole region (cf. Fig. 1). It can also be seen that from Fig. 1 if there is no real roots, then the region belongs to the naked singularity. An ergoregion is a region outside the event horizon where the time-like Killing vectors behave like space-like. A particle can enter into the ergoregion and leave again, and it moves in the direction of spin of the black hole and has relevance with the energy extraction process [44]. We have plotted the ergoregion

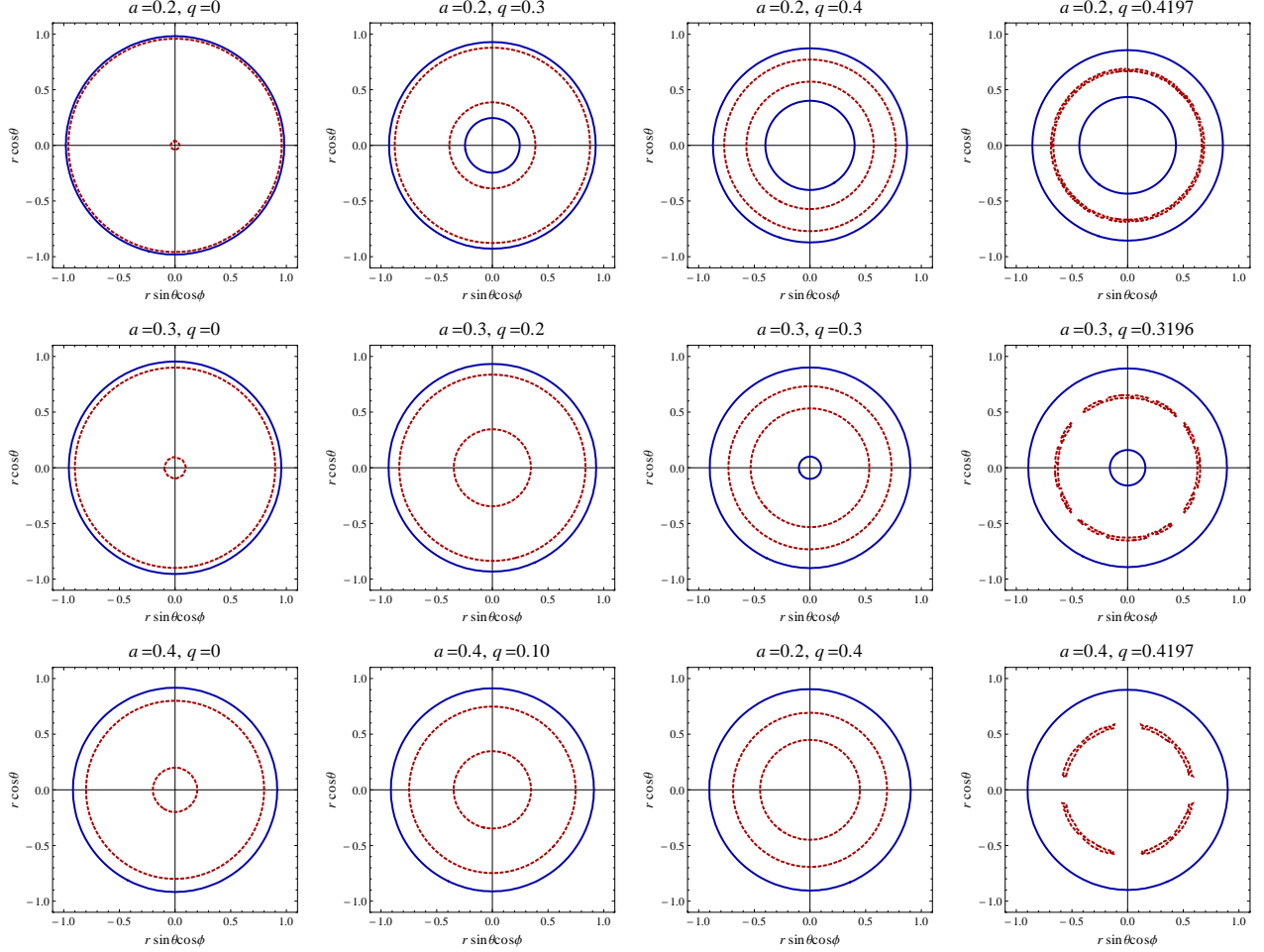


FIG. 2: The cross section of the event horizon, static limit surface, and ergosphere for different values of q for a fixed rotation parameter a . The blue line indicates static limit surface and the red one represents horizons.

of the five-dimensional EMCS black hole in Fig. 2 for different values of a and q . Figure 2 shows that there is an increase in the area of ergoregion when we increase the values of the parameter q and a . In Kerr black hole case, we known the region between event horizon and static limit surface as ergosphere, which can be seen from the Fig. 2. In Fig. 2, we explicitly bring out the effect of parameter q on the ergosphere, which shows that the area of the ergosphere grows with rotation parameter a as well as with q . Thus, for the faster rotating black holes its ergosphere also enlarges. The Fig. 2 suggests that the ergosphere area is maximum for an extremal five-dimensional EMCS black hole.

III. PARTICLE MOTION

In this section, we would like to study the shadow of EMCS black hole, which requires the complete study of particle motion around the black hole, and can be obtained by Hamilton-Jacobi formalism originally suggested by Carter [45]. The Hamilton-Jacobi equation [10] for the five-dimensional EMCS black hole (3) with the metric tensor $g_{\mu\nu}$ (6) reads:

$$-\frac{\partial S}{\partial \sigma} = \frac{1}{2} g^{\mu\nu} \frac{\partial S}{\partial x^\mu} \frac{\partial S}{\partial x^\nu}, \quad (26)$$

where σ is the affine parameter and S is the Jacobian action with the following separable ansatz for the Jacobian action [38]

$$S = \frac{1}{2} m_0 \sigma - Et + S_r(r) + S_\theta(\theta) + L_\phi \phi + L_\psi \psi, \quad (27)$$

where m_0 is the mass of the test particle which is zero for the photon case. $S(r)$ and $S(\theta)$ are respectively function of r and θ only. It can be seen that with Eq. (27) into Eq. (26), one can find the complete geodesic equations for the five-dimensional EMCS black hole [41]

$$\begin{aligned} \rho^2 \frac{dt}{d\sigma} = & E\rho^2 + \frac{1}{\Delta} \left[(M\zeta\gamma - q^2(\zeta + b^2) E \right. \\ & \left. + (a\gamma M + b\gamma q - aq^2) L_\phi + (\zeta bM + a\zeta q - bq^2) L_\psi \right], \end{aligned} \quad (28)$$

$$\begin{aligned} \rho^2 \frac{d\phi}{d\sigma} = & \frac{L_\phi}{\sin^2 \theta} - \frac{1}{\Delta} \left[((a^2 - b^2)\gamma + Mb^2 + 2abq) L_\phi \right. \\ & \left. + (Mab + (a^2 + b^2)q) L_\psi + (a\gamma M + b\gamma q - aq^2) E \right], \end{aligned} \quad (29)$$

$$\begin{aligned} \rho^2 \frac{d\psi}{d\sigma} = & \frac{L_\psi}{\cos^2 \theta} - \frac{1}{\Delta} \left[(-(a^2 - b^2)\zeta + Ma^2 + 2abq) L_\psi \right. \\ & \left. + (\zeta bM + a\zeta q - bq^2) E + (Mab + (a^2 + b^2)q) L_\phi \right], \end{aligned} \quad (30)$$

$$\rho^2 \frac{dx}{d\sigma} = \pm \sqrt{\mathcal{R}}, \quad (31)$$

$$\rho^2 \frac{d\theta}{d\sigma} = \pm \sqrt{\Theta}. \quad (32)$$

where $\zeta = x + a^2$ and $\gamma = x + b^2$. In the geodesic Eqs. (31) and (32), the terms \mathcal{R} and Θ are given by

$$\mathcal{R} = 4(E^2 \Delta x - \Delta \mathcal{K} + \mathcal{E} + \mu \mathcal{M} + 2q\mathcal{Q} - q^2 \mathcal{P}), \quad (33)$$

$$\Theta = E^2 (a^2 \cos^2 \theta + b^2 \sin^2 \theta) + \mathcal{K} - \frac{L_\phi^2}{\sin^2 \theta} - \frac{L_\psi^2}{\cos^2 \theta}, \quad (34)$$

where \mathcal{K} is Carter constant [45], and

$$\begin{aligned}\mathcal{E} &= (a^2 - b^2)(\gamma L_\phi^2 - \zeta L_\psi^2), \quad \mathcal{Q} = ab(L_\phi^2 + L_\psi^2) + (a^2 + b^2)L_\phi L_\psi + Eab\left(\frac{L_\phi\gamma}{a} + \frac{L_\psi\zeta}{b}\right), \\ \mathcal{M} &= \zeta\gamma E^2 + 2a\gamma EL_\phi + 2\zeta bEL_\psi + (bL_\phi + aL_\psi)^2, \quad \mathcal{P} = 2aEL_\phi + 2bEL_\psi + (\zeta + b^2)E^2.\end{aligned}$$

These equations define the geometry of photon around the spacetime of the five-dimensional EMCS black hole. For a particle moving in the equatorial plane and to remain in equatorial plane $\mathcal{K} = 0$ [46]. One can recover equation of motion for five-dimensional Myers-Perry black hole when $q = 0$ [38]. In the presence of a dark object behind a black hole and for obtaining the boundary of the black hole shadow it demands the study of radial equation. We can rewrite the radial equations of motion [25, 38]

$$\left(\frac{dx}{d\sigma}\right)^2 + V_{eff} = 0, \quad (35)$$

with the effective potential

$$V_{eff} = -\frac{4}{\rho^2} \left[E^2 \Delta x - \Delta \mathcal{K} + \mathcal{E} + \mu \mathcal{M} + 2q\mathcal{Q} - q^2 \mathcal{P} \right]. \quad (36)$$

If $q = 0$, the Eq. (36) reduces to

$$V_{eff} = -\frac{4}{\rho^2} \left[E^2 \Delta x - \Delta \mathcal{K} + \mathcal{E} + \mu \mathcal{M} \right], \quad (37)$$

which is the effective potential for the Myers-Perry black hole [47]. The apparent shape of the five-dimensional EMCS black hole can be obtained by the study of the photon orbits.

The impact parameters characterize the photon orbits around the black hole can be defines in terms of the constants of motion $\xi_1 = L_\phi/E$, $\xi_2 = L_\psi/E$ and $\eta = \mathcal{K}/E^2$. The expression for \mathcal{R} takes the form

$$\mathcal{R} = 4E^2 (\Delta x - \Delta \eta + \mu \mathcal{J} + 2q\mathcal{O} - q^2 \mathcal{S}), \quad (38)$$

where $\mathcal{J} = \zeta\gamma + 2a(\gamma\xi_1 + \zeta\xi_2) + a^2(\xi_1 + \xi_2)^2$, $\mathcal{O} = a^2(\xi_1^2 + \xi_2^2) + 2a^2\xi_1\xi_2 + a(\xi_1\gamma + \xi_2\zeta)$, and $\mathcal{S} = 2a(\xi_1 + \xi_2) + (\zeta + a^2)$. Henceforth, we assume that the two rotation parameters $a = b$.

Here we are interested in the radial motion of the photons, which are essential for determining the shadow of five-dimensional EMCS black hole. The spherical photon orbits, i.e., geodesics that stays on a sphere $r=\text{constant}$, defines the apparent shape of the black hole. The photons come from infinity and approaches to a turning point with zero radial velocity, which correspond to an unstable circular orbit determined by

$$V_{eff} = 0 \quad \text{and} \quad \frac{dV_{eff}}{dx} = 0, \quad \text{or} \quad \mathcal{R} = 0 \quad \text{and} \quad \frac{d\mathcal{R}}{dx} = 0. \quad (39)$$

By Eqs. (36) and (39), as in the Kerr case [48], one can obtain the parameters η and sum of parameters ξ_1, ξ_2 , which read

$$\begin{aligned} \eta = & \frac{1}{a(2q+1)(-1+2a^2+2x)^2} \left[2a^7(1+2q) + a^5[1+2q(3+3q+10x)+10x] \right. \\ & + 2a^3[q(1+q)(1+4q) + 2(-1+(-1+q)q)x + 7(1+2q)x^2] \\ & - 2(1+q)\sqrt{a^2(q^2+a^2(2+4q)+2x+4qx)(a^4+q^2+(-1+x)x+2a^2(q+x))^2} \\ & \left. + a(2q^3(1+q) + 4q^2(1+q)x - (5+2q(5+q))x^2 + 6(1+2q)x^3) \right], \end{aligned} \quad (40)$$

and

$$\begin{aligned} \xi_1 + \xi_2 = & \frac{1}{a^2(2q+1)(-1+2a^2+2x)} \left[-a^5(1+q) + a^3(1+3q+4q^2-2(1+q)x) \right. \\ & + a(q^3+2q^2x-(1+q)x^2) \\ & \left. - \sqrt{a^2(q^2+a^2(2+4q)+2x+4qx)(a^4+q^2+(-1+x)x+2a^2(q+x))^2} \right]. \end{aligned} \quad (41)$$

The impact parameters ξ_1, ξ_2 , and η for the photon orbits around five-dimensional EMCS black hole that determine the contour of the shadow [38]. Now we consider the case when $\theta = \pi/2$, $L_\psi = 0$, which implies $\xi_2 = 0$, therefore from Eq. (41), we obtain

$$\begin{aligned} \xi_1 = & \frac{1}{a^2(2q+1)(-1+2a^2+2x)} \left[-a^5(1+q) + a^3(1+3q+4q^2-2(1+q)x) \right. \\ & + a(q^3+2q^2x-(1+q)x^2) \\ & \left. - \sqrt{a^2(q^2+a^2(2+4q)+2x+4qx)(a^4+q^2+(-1+x)x+2a^2(q+x))^2} \right], \end{aligned} \quad (42)$$

and for $\theta = 0$, $L_\phi = 0$, which implies $\xi_1 = 0$, thus

$$\begin{aligned} \xi_2 = & \frac{1}{a^2(2q+1)(-1+2a^2+2x)} \left[-a^5(1+q) + a^3(1+3q+4q^2-2(1+q)x) \right. \\ & + a(q^3+2q^2x-(1+q)x^2) \\ & \left. - \sqrt{a^2(q^2+a^2(2+4q)+2x+4qx)(a^4+q^2+(-1+x)x+2a^2(q+x))^2} \right]. \end{aligned} \quad (43)$$

When charge is switch off ($q = 0$), then Eqs. (40) and (41) reduce to

$$\eta = \frac{(x+a^2)[2a^4+x(-5+6x)+a^2(1+8x)]+2[x-(x+a^2)^2]\sqrt{2(x+a^2)}}{(-1+2a^2+2x)^2}, \quad (44)$$

$$\xi_1 + \xi_2 = \frac{[a^2-(x+a^2)^2]+[x-(x+a^2)^2]\sqrt{2(x+a^2)}}{a(-1+2a^2+2x)}, \quad (45)$$

which are same as obtain for five-dimensional Myers-Perry black hole [38].

IV. BLACK HOLE SHADOW

Our aim is to calculate the boundary curve of the shadow and the existence of a photon surface around the EMCS black hole is necessary for the shadow. A black hole casts a shadow when it is situated between an observer at infinity and a bright object. The incoming photons toward the black hole may follow three possible trajectories, either it will fall into the black hole or it will be scattered away from the black hole and the other third possibility to obtain the critical geodesics which is the circular orbit around a black hole at critical radius. To visualize the apparent shape of the black hole, we use celestial coordinates α and β , which can be calculated by defining the orthonormal basis vectors [49] for the local observer

$$\begin{aligned} e_{\hat{t}} &= \lambda e_t + \varsigma e_\phi + \chi e_\psi, \\ e_{\hat{r}} &= \frac{1}{\sqrt{g_{rr}}} e_r, \quad e_{\hat{\theta}} = \frac{1}{\sqrt{g_{\theta\theta}}} e_\theta, \\ e_{\hat{\phi}} &= \frac{1}{\sqrt{g_{\phi\phi}}} e_\phi, \quad e_{\hat{\psi}} = \frac{1}{\sqrt{g_{\psi\psi}}} e_\psi, \end{aligned} \quad (46)$$

The coefficient in Eq. (46) are real and one can verify that $\{e_t, e_r, e_\theta, e_\phi, e_\psi\}$ are orthonormal [49]. Both local and the basis vectors of the metric (3) are related by the following relation:

$$e_{\hat{i}} = e_i^\mu e_\mu, \quad \text{and} \quad e_{\hat{i}}^\mu e_{\hat{j}}^\nu g_{\mu\nu} = \eta_{\hat{i}\hat{j}}, \quad (47)$$

where $\eta_{\hat{i}\hat{j}} = (-1, 1, 1, 1, 1)$. With the help of Eq. (46), (47) and using the orthonormal condition of the basis vectors, one can obtain the constants λ, ς, χ in the following form:

$$\begin{aligned} \lambda &= \frac{\sqrt{g_{\phi\psi}^2 - g_{\phi\phi}g_{\psi\psi}}}{\sqrt{g_{tt}g_{\phi\phi}g_{\psi\psi} + 2g_{t\phi}g_{t\psi}g_{\phi\psi} - g_{t\phi}^2g_{\psi\psi} - g_{t\psi}^2g_{\phi\phi} - g_{\phi\psi}^2g_{tt}}}, \\ \varsigma &= \frac{g_{t\phi}g_{\psi\psi} - g_{t\psi}g_{\phi\psi}}{\sqrt{g_{tt}g_{\phi\phi}g_{\psi\psi} + 2g_{t\phi}g_{t\psi}g_{\phi\psi} - g_{t\phi}^2g_{\psi\psi} - g_{t\psi}^2g_{\phi\phi} - g_{\phi\psi}^2g_{tt}}}, \\ \chi &= \frac{g_{t\phi}g_{\phi\psi} - g_{t\psi}g_{\phi\phi}}{\sqrt{g_{tt}g_{\phi\phi}g_{\psi\psi} + 2g_{t\phi}g_{t\psi}g_{\phi\psi} - g_{t\phi}^2g_{\psi\psi} - g_{t\psi}^2g_{\phi\phi} - g_{\phi\psi}^2g_{tt}}}, \end{aligned} \quad (48)$$

where the metric components are defined in Eq. (6). Further, the contravariant component of the three-momenta in the new coordinate basis [49] are given by

$$\begin{aligned}
p^{\hat{t}} &= \lambda E - \varsigma L_1 - \chi L_2, \\
p^{\hat{\phi}} &= \frac{1}{\sqrt{g_{\phi\phi}}} L_1, \\
p^{\hat{\psi}} &= \frac{1}{\sqrt{g_{\psi\psi}}} L_2, \\
p^{\hat{\theta}} &= \frac{p_\theta}{\sqrt{g_{\theta\theta}}} = \frac{\pm\sqrt{\Theta}}{\sqrt{g_{\theta\theta}}}.
\end{aligned} \tag{49}$$

To describe the black hole shadow, we introduce the celestial coordinates [49]:

$$\begin{aligned}
\alpha &= \lim_{r_0 \rightarrow \infty} -r_0 \frac{(p^{\hat{\phi}} + p^{\hat{\psi}})}{p^{\hat{t}}}, \\
\beta &= \lim_{r_0 \rightarrow \infty} r_0 \frac{p^{\hat{\theta}}}{p^{\hat{t}}}.
\end{aligned} \tag{50}$$

Here we take limit $r \rightarrow \infty$ because an observer is far away from the black hole, and θ_0 is the angular coordinate of the observer or the inclinations angle. Substituting the contravariant components of three-momenta from Eq. (49) in Eq. (50), the celestial coordinates take the form

$$\begin{aligned}
\alpha &= -(\xi_1 \csc \theta_0 + \xi_2 \sec \theta_0), \\
\beta &= \pm \sqrt{\eta - \xi_1^2 \csc^2 \theta_0 - \xi_2^2 \sec^2 \theta_0 + a^2}.
\end{aligned} \tag{51}$$

Interestingly, Eq. (51) has the same form as five-dimensional Myers-Perry black hole [38] with modified impact parameters η and $\xi_1 + \xi_2$ given respectively by Eqs. (40) and (41). However, the Eq. (51) has different form from the Kerr-Newman black hole [11] with additional terms due to extra dimension. Now we consider the case when an observer is situated in the equatorial plane of the five-dimensional EMCS black hole, i.e., the inclination angle is $\theta_0 = \pi/2$. In this case, the impact parameter $L_\psi = 0$ therefore $\xi_2 = 0$, hence the Eq. (51) transforms to

$$\begin{aligned}
\alpha &= -\xi_1, \\
\beta &= \pm \sqrt{\eta - \xi_1^2 + a^2}.
\end{aligned} \tag{52}$$

Similarly for $\theta_0 = 0$, in this case $L_\phi = 0$ and hence $\xi_1 = 0$,

$$\begin{aligned}
\alpha &= -\xi_2, \\
\beta &= \pm \sqrt{\eta - \xi_2^2 + a^2}.
\end{aligned} \tag{53}$$

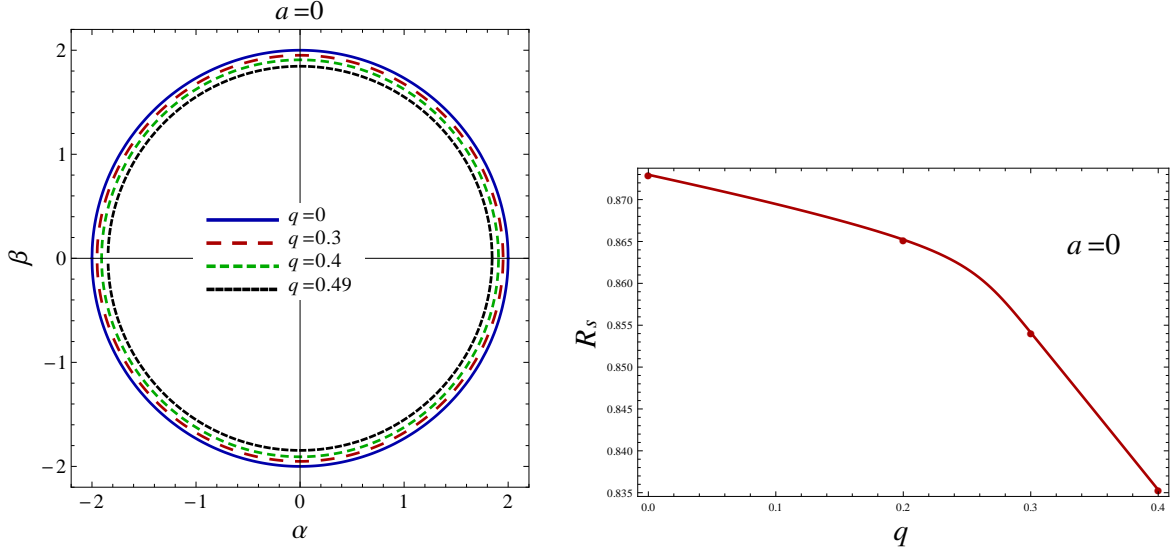


FIG. 3: Plot showing the shapes of black hole shadow cast by EMCS black hole with inclination angle $\theta_0 = \pi/2$, for different values of charge q and spin $a = 0$.

The shadows of a five-dimensional EMCS black hole can be visualized by plotting α vs β for different values of the rotation parameter (a) and the charge (q) at different inclination angles. One can check that the celestial coordinates α and β in Eqs. (52) and (53) will satisfy the following relation $\alpha^2 + \beta^2 = \eta + a^2$, where η is given by Eq. (40). Equation (53) depends on charge q and spin a and also due to extra dimension.

The shadow with $a = 0$ of a five-dimensional nonrotating black hole can be obtain from

$$\alpha^2 + \beta^2 = \frac{2 - 9q^2 + 2(1 - 3q^2)^{3/2}}{1 - 4q^2} \equiv r_s^2 \quad \text{with} \quad x = 1 + \sqrt{(1 - 3q^2)}. \quad (54)$$

The nonrotating five-dimensional EMCS black hole is a general case of five-dimensional Reissner-Nordström black hole and its shadow appears as a perfect circle with radius r_s depicted in Fig. 3. We plotted the shadow of a nonrotating five-dimensional EMCS black hole for several decreasing values of charge q . The effect of charge q can be seen with the radius of the circle with an increase in q (cf. Fig. 3). The case when $q = 0$ gives the radius of the circle is 2, which is a five-dimensional Schwarzschild black hole [39]. Thus the effect of positive q is to decrease the size of the shadow (cf. Fig. 3).

Now we consider the rotating case of the five-dimensional EMCS black hole to see the behavior of black hole shadow in the presence of both spin a , charge q , and extra dimension. The celestial coordinates in the rotating case satisfy the relation, $\alpha^2 + \beta^2 = \eta + a^2$. With

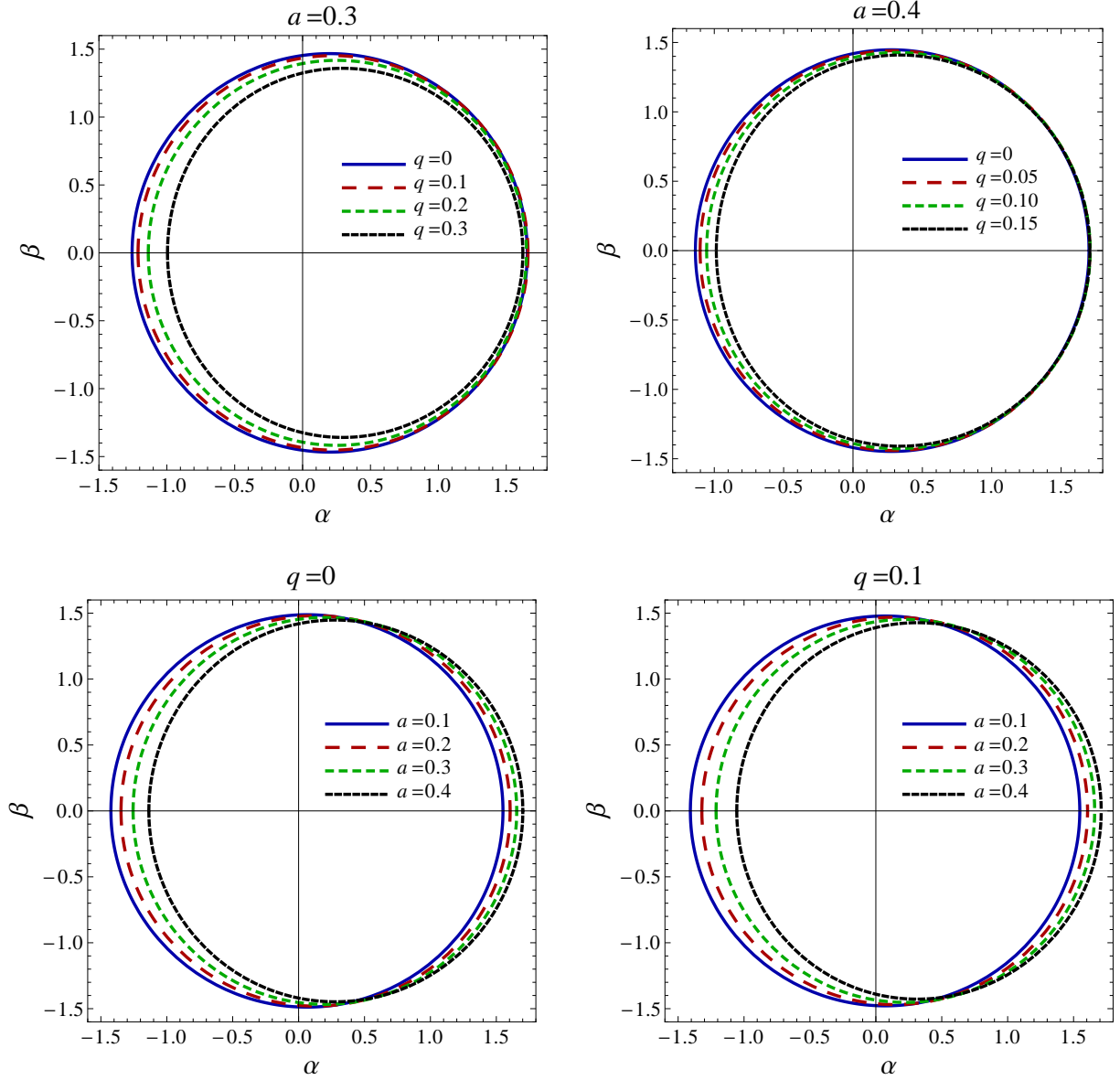


FIG. 4: Plot showing the shapes of black hole shadow cast by EMCS black hole with inclination angle $\theta_0 = \pi/2$ for different values of charge q and spin a .

increasing a , the shadow gets more and more distorted and shifts to rightmost on vertical axis. If we calculate the celestial coordinate relation in the absence of charge, i.e., $q = 0$

$$\alpha^2 + \beta^2 = \frac{(x + a^2) [2a^4 + x(-5 + 6x) + a^2(1 + 8x)] + 2(x - (x + a^2)^2) \sqrt{2(x + a^2)}}{(-1 + 2a^2 + 2x)^2} + a^2. \quad (55)$$

The shape of five-dimensional EMCS black hole have been plotted in Fig. 4 for different values of charge q and spin a . The shape of the black hole shadow is a deformed circle

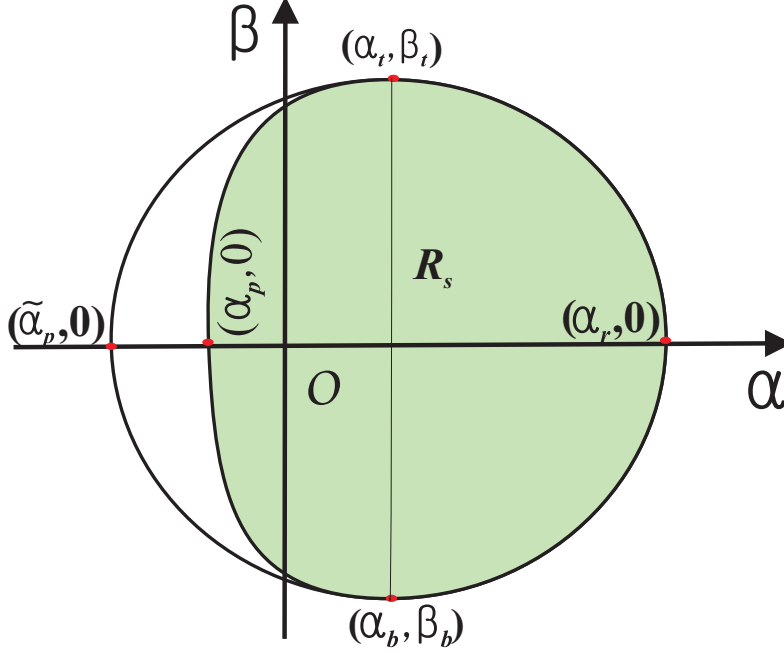


FIG. 5: Schematic representation of the observables for rotating black holes [14].

instead of being a perfect circle. We see that the shape of the shadow is largely affected due to the parameters a , q and extra dimension. The size of the shadow decreases continuously (cf. Fig. 4) with increase in q . This can be understood as a dragging effect due to the rotation of the black hole. The extra dimension also have an effect on size of the shadow [38]. However, the shape of a shadow is more relevant with the size [50].

Next, it will be helpful to introduce observables, which characterize the shape and the distortion of the shadow. We consider the Hioki-Maeda characterization [48] to determine observables, i.e., radius R_s and deformation δ_s , for rotating five-dimensional EMCS black hole [17, 48]:

$$R_s = \frac{(\alpha_t - \alpha_r)^2 + \beta_t^2}{2(\alpha_t - \alpha_r)}, \quad (56)$$

and

$$\delta_s = \frac{\tilde{\alpha}_p - \alpha_p}{R_s}, \quad (57)$$

where $(\tilde{\alpha}_p, 0)$ and $(\alpha_p, 0)$ are the coordinates where the reference circle and the contour of the shadow cut the horizontal axis on the opposite side of $(\alpha_r, 0)$ (cf. Fig. 5). In this characterization, the idea was that a reference circle is passing through the three coordinates of the black hole shadow. Apart from it, there is another characterization of the observables

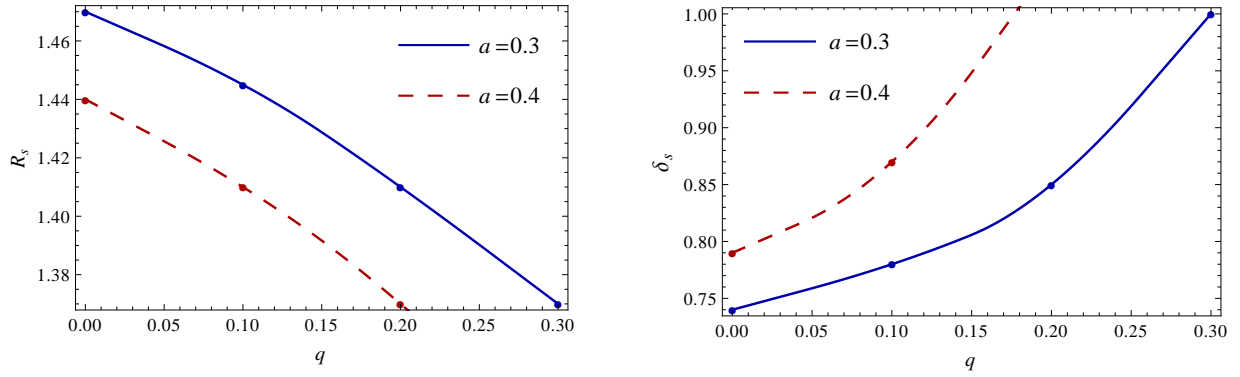


FIG. 6: Plots showing the variation of radius of black hole shadow R_s and distortion parameter δ_s with charge q for different value of spin a .

to extract the same information from the black hole shadow [21]. The coordinates are situated at top position (α_t, β_t) , bottom position (α_b, β_b) , and rightmost position $(\alpha_r, 0)$ (cf. Fig. 5). The behavior of radius R_s and distortion δ_s with charge for different values of spin a is depicted in Fig. 6. Figure 6 suggests that the radius R_s monotonically decreases as q increases, and the distortion δ_s of the shadow increase with q and the shadow gets more distortion for larger values of a (cf. Fig. 6). When compared with the five-dimensional Myers-Perry black hole [38], the effective size of the shadow decreases for higher values of charge q . Also, a comparison of the shadow with Kerr-Newman black hole [11] indicates that the effective size of the shadow decreases due to the extra dimensions. Instead of using R_s and δ_s , one can also use observables defined by Schee and Stuchlík [21] to get same form.

V. NAKED SINGULARITY

The cosmic censorship hypothesis states that the spacetime singularities are always hidden by the event horizon of the black hole [51]. However, a naked singularity can be defined as a gravitational singularity in the absence of the event horizon, which lead to the violation of cosmic censorship hypothesis [51]. Recently, Figueras *et al.* [52] have found the strongest evidence for the violation of the weak cosmic conjecture in five-dimensional spacetime. Hence, it is important to study the naked singularity shadow for the five-dimensional EMCS black hole.

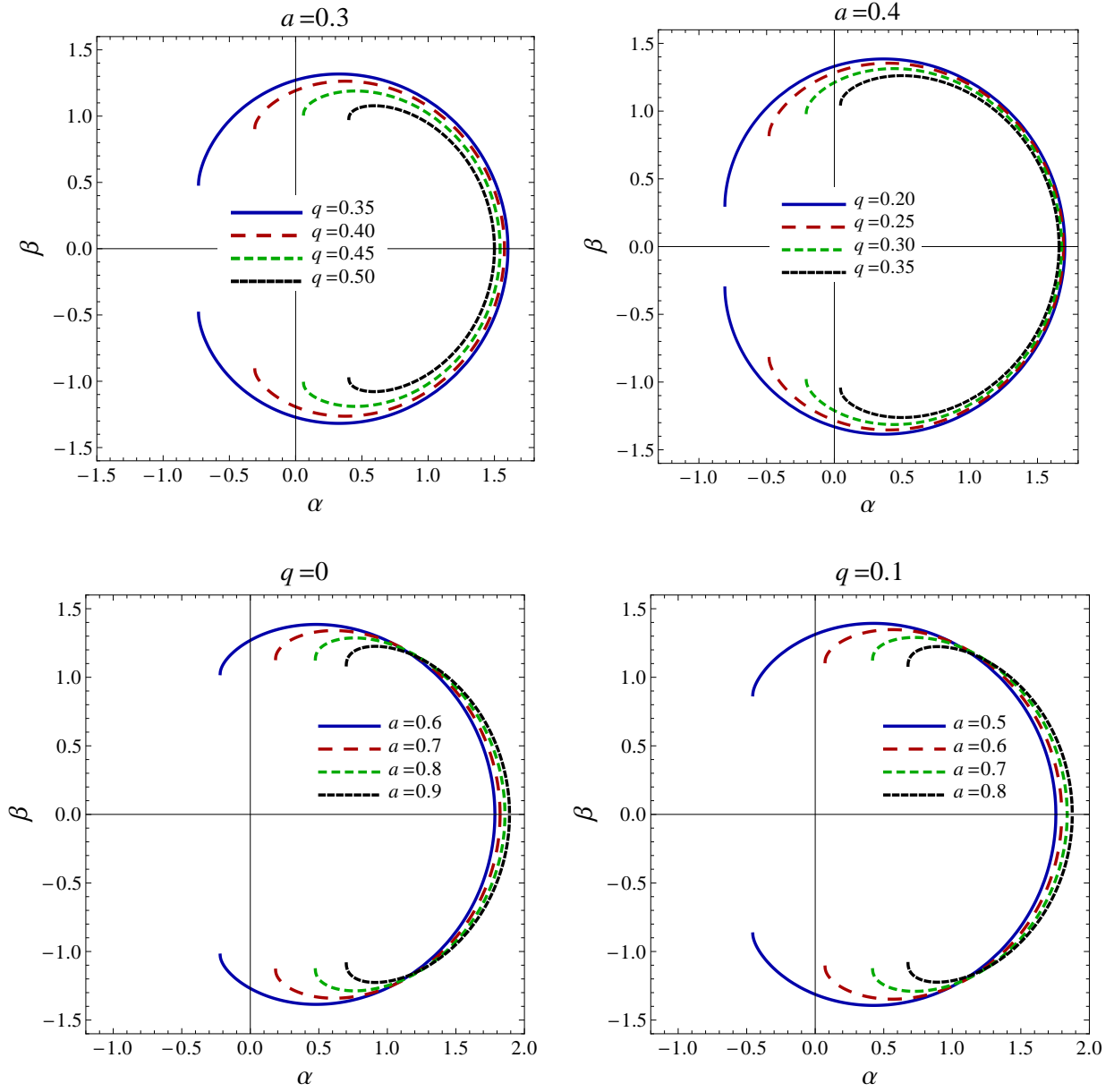


FIG. 7: Shadow cast by the naked singularity with inclination angle $\theta_0 = \pi/2$ for different values of the charge q and spin a .

A five-dimensional EMCS black hole admits a naked singularity, it occurs when $\mu < (a+b)^2 + 2q$ or for the case of $a = b$, $\mu < 2(2a^2 + q)$. In the absence of charge q , the condition for the existence of the naked singularity satisfy $\mu < (a+b)^2$ ($a \neq b$) and $\mu < 4a^2$ ($a = b$) or $a > 1/\sqrt{2}$, which is most general condition for naked singularity in five-dimensional Myers-Perry spacetime [38]. The shadow of naked singularity for five-dimensional Myers-Perry spacetime is studied in [38].

Here we plot the contour of the naked singularity shadow for different values of q and a in Fig. 7, and the shape changes dramatically with respect to black hole shadow. It is found that the shape of a naked singularity shadow forms an arc instead of a circle (cf. Fig. 7). The arc shape occurs due to the absence of the event horizon. The shape of the naked singularity shadow is affected by charge q as well as spin a ; its arc size decreases in both the cases when we increase either q or a (cf. Fig. 7). Our results show that the naked singularity shadow is different from the five-dimensional Myers-Perry black hole [38] (cf. Fig. 7). We demonstrate that the naked singularity shadow is smaller in size as compare to the five-dimensional Myers-Perry black hole (cf. Fig. 7).

VI. ENERGY EMISSION RATE

In this section, we study the energy emission rate of a five-dimensional EMCS black hole. It is known that the shadow is responsible for high energy absorption cross section due to the black hole for a far away observer. The energy emission rate of a black hole can be calculated via using the following relation [25, 53, 54]:

$$\frac{d^2 E(\omega)}{d\omega dt} = \frac{2\pi^2 \sigma_{lim}}{\exp(\omega/T) - 1} \omega^3, \quad (58)$$

where ω is frequency, σ_{lim} is the limiting constant value for a spherically symmetric black hole around which the absorption cross section oscillates, and T is Hawking temperature. If one calculates the Hawking temperature of five-dimensional EMCS black hole [55]

$$T = \frac{x_+^2 - (a^2 + q)^2}{2\pi\sqrt{x_+}[a^2 q + (x_+ + a^2)^2]}, \quad (59)$$

where x_+ is the event horizon. Interestingly, the Hawking temperature (59) depends on charge q as well as spin a . When $q \rightarrow 0$, the temperature reduces to

$$T = \frac{x_+ - a^2}{2\pi\sqrt{x_+}(x_+ + a^2)}, \quad (60)$$

which shows the temperature of the Myers-Perry black holes [56]. The limiting constant value of a five-dimensional EMCS black hole can be expressed approximately [53, 54]

$$\sigma_{lim} \approx \pi R_s^3, \quad (61)$$

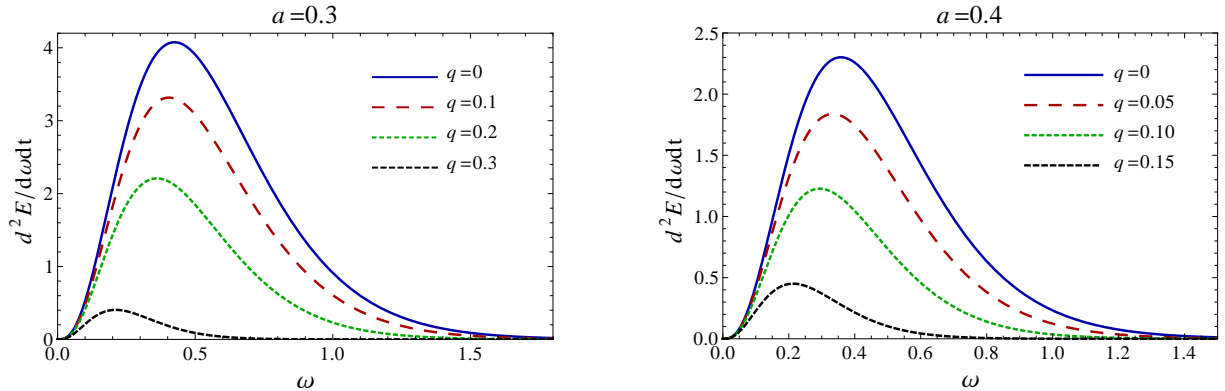


FIG. 8: Plots showing the variation of the energy emission rate with frequency ω for different values of charge q and spin a .

where R_s is the radius of the black hole shadow. Hence, the complete form of energy emission rate for five-dimensional EMCS black hole is

$$\frac{d^2 E(\omega)}{d\omega dt} = \frac{4\pi^3 R_s^3}{e^{\omega/T} - 1} \omega^3. \quad (62)$$

In Fig. 8, we plot the energy emission rate versus frequency ω for different value of charge q and spin a . It can be seen that with an increase in the value of q and a decreases the peak of energy emission rate (cf. Fig. 8). We analyze that the energy emission rate of a five-dimensional EMCS black hole decreases in comparison with a five-dimensional Myers-Perry black hole [38].

VII. CONCLUSION

The formation of shadow due to the strong gravitational field effects near black holes has received significant attention due to a possibility of observing the images of Sgr A* [6]. The gravitational theories with extra dimensions admit black hole solutions which have different properties than standard ones. Several tests were proposed to discover signatures of extra dimensions in black holes as the gravitational field likely to be distinct from the one in general relativity, e.g., the gravitational lensing for gravities with extra dimensions has different characteristics than in general relativity. It turns out that the measurements of the shadow sizes for higher-dimensional black holes can put constraints on parameters of the black holes [57], e.g., evaluating the size of shadow, it was shown that the probability to tidal charge ($-q$) for the black hole at the Galactic Center is ruled out by observations [58].

Thus, it suggests that a black hole with positive charge q is consistent with observations but a significant negative $-q$ black holes are ruled out [58], i.e., the Reissner-Nordström black holes which have positive charge q are consistent with observations, but not the Brane-World black holes which have a negative tidal charge $-q$.

The five-dimensional EMCS black hole solution has an additional charge parameter q than the five-dimensional Myers-Perry black hole, and it gives deviation from the Myers-Perry black hole but the black hole has a richer configuration for the horizons and ergosphere. It is interesting to see that the ergosphere size is sensitive to the charge q as well as to rotation parameter a . We have extended the previous studies of the black hole shadow and derived analytical formulas for the photon regions of shadow for a five-dimensional EMCS black hole. We also make quantitative analyses of the shape and size of the black hole shadow cast by a rotating five-dimensional EMCS black hole considering the various parameters. Moreover, we have analyzed how the shadow of the black hole is changed by the presence of charge q and we explicitly show that the charge q apparently affects the shape and the size of the shadow. In particular, the shadow of a rotating five-dimensional EMCS black is found to be a dark zone covered by a deformed circle. For a fixed value of spin a compared to the rotating five-dimensional Myers-Perry black hole; the size of the shadow decreases with the charge q whereas shadows become more distorted with an increase in charge q , and the distortion is maximal for an extremal black hole. In a comparison with the four-dimensional Kerr-Newman black hole, we found that the shadow of five-dimensional EMCS black hole decreases due to the higher-dimensional effect. The naked singularity shadow of a five-dimensional EMCS metric suggests that the shape of the shadow decreases for higher values of the charge q when compared with a five-dimensional Myers-Perry naked singularity shadow. It may be interesting to check observationally whether the size of the shadow suggest if there are signatures of a five-dimensional charged black hole.

Acknowledgments

M.A. acknowledges the University Grant Commission, India, for financial support through the Maulana Azad National Fellowship For Minority Students scheme (Grant No. F1-17.1/2012-13/MANF-2012-13-MUS-RAJ-8679). S.G.G. would like to thank SERB-DST Research Project Grant No. SB/S2/HEP-008/2014 and DST INDO-SA bilateral project

- [1] A. de Vries, *Class. Quant. Grav.* **17**, 123 (2000).
- [2] R. Takahashi, *J. Korean Phys. Soc.* **45**, S1808 (2004) [*Astrophys. J.* **611**, 996 (2004)].
- [3] C. Bambi and K. Freese, *Phys. Rev. D* **79**, 043002 (2009).
- [4] C. Bambi and N. Yoshida, *Class. Quant. Grav.* **27**, 205006 (2010).
- [5] C. Goddi *et al.*, *Int. J. Mod. Phys. D* **26**, 1730001 (2016).
- [6] H. Falcke, F. Melia and E. Agol, *Astrophys. J.* **528**, L13 (2000).
- [7] J.M. Bardeen, in *Black holes, in Proceedings of the Les Houches Summer School, Session 215239*, edited by C. De Witt and B.S. De Witt (Gordon and Breach, New York, 1973).
- [8] J.L. Synge, *Mon. Not. Roy. Astron. Soc.* **131**, 463 (1963).
- [9] J.P. Luminet, *Astron. Astrophys.* **75**, 228 (1979).
- [10] S. Chandrasekhar, *The Mathematical Theory of Black Holes* (Oxford University Press, New York, 1992).
- [11] R. Takahashi, *Publ. Astron. Soc. Jap.* **57**, 273 (2005).
- [12] Z. Li and C. Bambi, *J. Cosmol. Astropart. Phys.* 01 (2014) 041.
- [13] A. Abdujabbarov, M. Amir, B. Ahmedov and S.G. Ghosh, *Phys. Rev. D* **93**, 104004 (2016).
- [14] M. Amir and S.G. Ghosh, *Phys. Rev. D* **94**, 024054 (2016).
- [15] A. Yumoto, D. Nitta, T. Chiba and N. Sugiyama, *Phys. Rev. D* **86**, 103001 (2012).
- [16] L. Amarilla, E.F. Eiroa and G. Giribet, *Phys. Rev. D* **81**, 124045 (2010).
- [17] L. Amarilla and E. F. Eiroa, *Phys. Rev. D* **85**, 064019 (2012).
- [18] A. Grenzebach, V. Perlick and C. Lämmerzahl, *Phys. Rev. D* **89**, 124004 (2014).
- [19] A. Abdujabbarov, F. Atamurotov, Y. Kucukakca, B. Ahmedov and U. Camci, *Astrophys. Space Sci.* **344**, 429 (2013).
- [20] K. Hioki and U. Miyamoto, *Phys. Rev. D* **78**, 044007 (2008).
- [21] J. Schee and Z. Stuchlik, *Int. J. Mod. Phys. D* **18**, 983 (2009).
- [22] L. Amarilla and E. F. Eiroa, *Phys. Rev. D* **87**, 044057 (2013).
- [23] F. Atamurotov, A. Abdujabbarov and B. Ahmedov, *Astrophys. Space Sci.* **348**, 179 (2013).
- [24] F. Atamurotov, A. Abdujabbarov and B. Ahmedov, *Phys. Rev. D* **88**, no. 6, 064004 (2013).
- [25] S.W. Wei and Y.X. Liu, *J. Cosmol. Astropart. Phys.* 11 (2013) 063.

- [26] A. A. Abdujabbarov, L. Rezzolla and B. J. Ahmedov, Mon. Not. Roy. Astron. Soc. **454**, 2423 (2015).
- [27] Z. Younsi, A. Zhidenko, L. Rezzolla, R. Konoplya and Y. Mizuno, Phys. Rev. D **94**, 084025 (2016).
- [28] G.T. Horowitz and T. Wiseman, arXiv:1107.5563.
- [29] N. Arkani-Hamed, S. Dimopoulos and G.R. Dvali, Phys. Lett. B **429**, 263 (1998).
- [30] I. Antoniadis, N. Arkani-Hamed, S. Dimopoulos and G. R. Dvali, Phys. Lett. B **436**, 257 (1998).
- [31] L. Randall and R. Sundrum, Phys. Rev. Lett. **83**, 3370 (1999).
- [32] R. Emparan and H.S. Reall, Living Rev. Rel. **11**, 6 (2008).
- [33] T. Adamo and E. T. Newman, Scholarpedia **9**, 31791 (2014).
- [34] H.S. Reall, Phys. Rev. D **68**, 024024 (2003).
- [35] R.C. Myers and M.J. Perry, Annals Phys. **172**, 304 (1986).
- [36] Z.-W. Chong, M. Cvetič, H. Lu and C.N. Pope, Phys. Rev. Lett. **95**, 161301 (2005).
- [37] J.P. Gauntlett, J.B. Gutowski, C.M. Hull, S. Pakis and H.S. Reall, Class. Quant. Grav. **20**, 4587 (2003).
- [38] U. Papnoi, F. Atamurotov, S. G. Ghosh and B. Ahmedov, Phys. Rev. D **90**, 024073 (2014).
- [39] B.P. Singh and S.G. Ghosh, arXiv:1707.07125.
- [40] E. Cremmer, *Supergravities in 5 Dimensions*, in *Superspace and supergravity, Proceedings of Nuffield Workshop*, Cambridge University Press, Cambridge U.K. (1980), page 267.
- [41] S. Paranjape and S. Reimers, Phys. Rev. D **94**, 124003 (2016).
- [42] J. M. Maldacena, Int. J. Theor. Phys. **38**, 1113 (1999).
- [43] F. R. Tangherlini, Nuovo Cim. **27**, 636 (1963).
- [44] R. Penrose and R.M. Floyd, Nature Physical Science **229**, 177 (1971).
- [45] B. Carter, Phys. Rev. **174**, 1559 (1968).
- [46] J. M. Bardeen, W. H. Press and S. A. Teukolsky, Astrophys. J. **178**, 347 (1972).
- [47] V.P. Frolov and D. Stojkovic, Phys. Rev. D **68**, 064011 (2003).
- [48] K. Hioki and K. i. Maeda, Phys. Rev. D **80**, 024042 (2009).
- [49] T. Johannsen, Astrophys. J. **777**, 170 (2013).
- [50] A. Grenzebach, *The Shadow of Black Holes: An Analytic Description*, SpringerBriefs in Physics, Springer, Heidelberg (2016).

- [51] R. Penrose, Riv. Nuovo Cim. **1**, 252 (1969) [Gen. Rel. Grav. **34**, 1141 (2002)].
- [52] P. Figueras, M. Kunesch and S. Tunyasuvunakool, Phys. Rev. Lett. **116**, 071102 (2016).
- [53] B. Mashhoon, Phys. Rev. D **7**, 2807 (1973).
- [54] C.W. Misner, K.S. Thorne and J.A. Wheeler, *Gravitation*, Freeman, San Francisco (1973).
- [55] S.Q. Wu, Phys. Rev. D **80**, 044037 (2009).
- [56] N. Altamirano, D. Kubiznak, R. B. Mann and Z. Sherkatghanad, Galaxies **2**, 89 (2014).
- [57] A.F. Zakharov, F. De Paolis, G. Ingrosso, A.A. Nucita, New Astronomy Reviews **56**, 64 (2012).
- [58] S.S. Doeleman *et al.*, Nature **455**, 78 (2008).